Progress in Organic Coatings 125 (2018) 530–536

Contents lists available at ScienceDirect

Progress in Organic Coatings

journal homepage: www.elsevier.com/locate/porgcoat

Wetting behavior of superhydrophobic poly(methyl methacrylate)

Emel Yilgör, Cagla Kosak Söz, Iskender Yilgör*

KUYTAM Surface Science and Technology Center, Chemistry Department, Koc University, Istanbul, Turkey

ARTICLE INFO

Keywords:
Superhydrophobic coating
PMMA surface
Cassie-Baxter model

ABSTRACT

Superhydrophobic PMMA surfaces were prepared by spin-coating and doctor blade coating of PMAA/hydrophobic silica (1/10 by weight) dispersions in toluene onto glass substrates. Influence of the number of coating layers applied and gauge thickness of the doctor blade used on surface properties were investigated. Formation of dual scale, micro/nano surface topographies were demonstrated by scanning electron microscopy, atomic force microscopy and white light interferometry studies. Roughness factor (r) and average surface roughness (R_a) values of the surfaces were determined. Wetting behavior of superhydrophobic PMMA surfaces obtained by introducing micro-nano, hierarchical roughness to inherently hydrophilic smooth PMMA films cannot be explained by Wenzel model. Therefore, wetting behavior of these surfaces were analyzed using Cassie-Baxter model and area fraction of surface protrusions were estimated.

1. Introduction

Poly(methyl methacrylate) (PMMA) films and sheets, which display excellent clarity and high transmission of visible light are widely used as protective panels in outdoor displays. PMMA is an inherently hydrophilic polymer which can be wetted by water or aqueous dirt that reduces its transparency and clarity. Such problems can be avoided by applying a thin, clear, superhydrophobic, self-cleaning coating on PMMA surfaces. As a result preparation, characterization and practical applications of superhydrophobic polymer surfaces have received broad interest from both academic and industrial research groups particularly due to their self-cleaning behavior [1–5]. Numerous methods have been developed for the preparation of superhydrophobic polymer surfaces [3,5–10]. Although it is possible to produce superhydrophobic surfaces by a large number of methods, in many cases they involve complex processes and use of specialized equipment and may be applicable to only specific polymers. Recently, we reported simple processes for the preparation of superhydrophobic polymer surfaces, which were based on spin-coating of hydrophobic silica onto various polymeric substrates [11,12]. Later on we also demonstrated preparation of superhydrophobic polymer surfaces by using silicone-urea copolymer/silica dispersions in organic solvents, which could be applied by spin coating, spraying or by a doctor blade [13]. Applicability of these methods to various thermoplastic polymers such as, polystyrene, polyurethanes and thermosetting systems, such as crosslinked epoxy resins were reported [11,13,14].

Theoretical models of wetting of rough surfaces by Wenzel [15] and Cassie-Baxter [16] have been developed long before the dramatic increase in the interest by synthetic scientists and application engineers for these systems, which followed the topographical characterization of various plant leaves and insect wings using scanning electron microscopy [17–19]. These studies led to a clear understanding of the critical structural and surface parameters in controlling the superhydrophobic behavior. Wettability of rough surfaces are generally explained by Wenzel [15] or Cassie-Baxter [16] models or their modified versions [20–25]. In Wenzel model, which assumes complete wetting of the rough surface as schematically shown in Fig. 1a, contact angle on a rough surface can be calculated using Eq. (1), where, (θ) and (θ_W) are the water contact angles measured on a smooth and rough surface respectively. The roughness factor (r) is the ratio of the actual area of a rough surface to its projected geometric area. By definition (r) is always greater than 1.

$$\mathrm{Cos}\theta_W = r \cdot \cos\theta \quad (1)$$

Unlike Wenzel, Cassie-Baxter model assumes the water droplet to sit on the protrusions (and air pockets) present on the surface, as shown schematically in Fig. 1b. In Cassie-Baxter model the contact angle on a rough surface (θ_{CB}) is calculated by using Eq. (2), where, (f) is the fraction of the surface on top of the protrusions, (1-f) is the fraction of air pockets, (θ) and (θ_g) are the water contact angles on smooth film surface and the air pockets respectively. If the water contact angle in air is assumed to be 180°, ($\cos 180 = -1$) then Eq. (3) is obtained.

$$\mathrm{Cos}\theta_{CB} = f \cdot \cos\theta + (1-f) \cdot \cos\theta_g \quad (2)$$

* Corresponding author.
E-mail address: iyilgor@ku.edu.tr (I. Yilgör).

https://doi.org/10.1016/j.porgcoat.2018.07.018
Received 30 May 2018; Received in revised form 4 July 2018; Accepted 12 July 2018
Available online 14 August 2018
0300-9440/

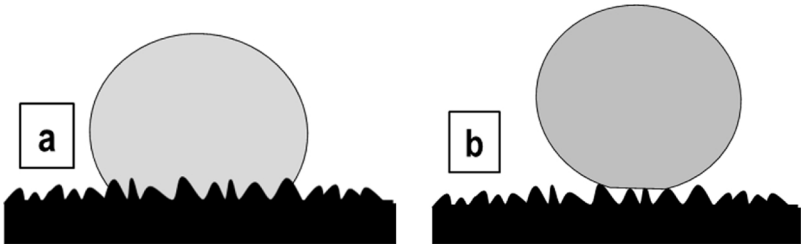

Fig. 1. Schematic representations of the wetting behavior of rough surfaces in; (a) Wenzel model and (b) Cassie-Baxter model.

$$\mathrm{Cos}\theta_{CB} = f \cdot \cos\theta + f - 1 \quad (3)$$

There is a continuing debate in the literature on the applicability of these theoretical models on the wetting behavior of rough surfaces and conditions necessary for their applications [21,22,24,26–28]. In this study we report preparation and characterization of superhydrophobic PMMA surfaces by spin-coating and doctor blade coating, using PMMA/silica dispersions in toluene. It is important to note that smooth PMMA film surfaces are hydrophilic with a static water contact angle (CA) of 67.5°. According to Wenzel model it is impossible to obtain hydrophobic PMMA surfaces by increasing the roughness factor (r). According to Wenzel Model formulated by Eq. (1), as (r) increases, ($\cos\theta_W$) will also increase, however the water contact angle (θ_W) will decrease, as shown in Fig. 2a.

Unlike the Wenzel approach, it is possible to obtain superhydrophobic PMMA surfaces in Cassie-Baxter model even though the smooth polymer surface is hydrophilic. As can be deduced from Eq. (3), as the surface area fraction of protrusions (f) decrease or fraction of air pockets (1-f) increase, ($\cos\theta_{CB}$) becomes more negative and contact angle (θ_{CB}) increases. This can easily be seen in Fig. 2b, where static water contact angles calculated from Cassie-Baxter relationship (Eq. (3)) are plotted against fraction of surface air pockets (1-f) for rough PMMA surfaces. Water contact angles greater than 150° (one of the requirements for superhydrophobic behavior) is obtained for PMMA surfaces when 1-f > 0.90, or in other words when protrusions constitute less than 10% of the total surface area.

2. Experimental

2.1. Materials

Hydrophobic fumed silica HDK H2000 (H2K) with a primary particle size in 5–30 nm range was provided by Wacker Chemie, Germany. Specific surface area of H2K is 150 m^2/g. Poly(methyl methacrylate) (PMMA) (M_n = 62,000, M_w = 138,000 g/mol) was prepared by free-radical polymerization in toluene solution in our laboratories. Reagent grade toluene (Merck) was used as received.

2.2. Coating processes

PMMA/silica (1/10 by weight) dispersions were prepared in toluene by dissolving 0.5 g of PMMA in 95 g of toluene followed by the addition of 5.0 g of silica. Mixture was stirred for 30 min by a magnetic stirrer and sonicated for 30 min to obtain homogeneous dispersions. Spin-coating was applied on a Model 7600 Spin-Coater by Specialty Coating Systems, Inc., Indianapolis, USA. Several drops of PMMA/silica dispersion was placed on a clean glass slide and spin-coated at 1000 rpm. The process was repeated to apply desired number of layers. Coated samples were dried at room temperature overnight and then in a vacuum oven at 50 °C for 24 h. Spin-coated samples were coded as follows: PMMA-SC-X, where SC indicated the spin-coating process and X showed the number of layers applied.

Doctor blade coating of PMMA/silica (1/10 by weight) dispersion in toluene was applied on glass substrates by using gauge thicknesses of 200, 125 and 50 µm. Coatings were dried overnight at room temperature and then in a vacuum oven at 40 °C for 24 h. Upon drying polymer film thicknesses obtained were approximately 5, 3 and 1.3 µm respectively. Doctor blade coated samples were coded as follows: PMMA-DB-X, where DB indicated the doctor blade coating process and X showed the gauge length.

2.3. Characterization methods

A field-emission Zeiss Ultra Plus Scanning Electron Microscope operated at 2–10 kV was used to investigate the PMMA/silica film surfaces, which were coated with a 2–3 nm layer of gold to minimize charging. 2D and 3D surface topographies of the surfaces were investigated by White Light Interferometry (WLI) on a Bruker Contour GT Motion 3D Microscope and non-contact surface profiler at the vertical scanning interferometry (VSI) mode. Surface roughness values were obtained by averaging 10 different surface maps with dimensions of 47 × 63 μm^2. Static water contact angle (CA) measurements were performed at 23 ± 2 °C using 5 µL droplets of deionized, triple distilled water on a Dataphysics OCA 35 goniometer equipped with SCA 20 software. An average of 10 contact angle readings were taken for each sample. Advancing water contact angles were determined by increasing the volume of the sessile drop from 5 µL to 25 µL at a rate of 0.2 µL/s.

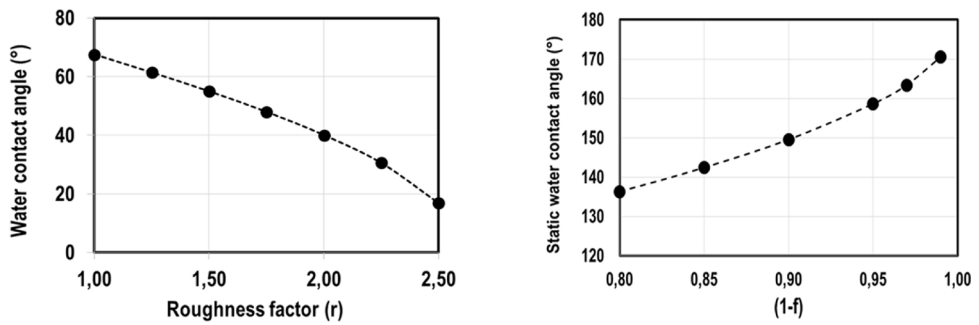

Fig. 2. (a) Change in the static water contact angle of PMMA surface as a function of roughness factor (r) according to Wenzel model. (b) Change in the static water contact angle of a rough PMMA surface as a function of the surface area fraction of air pockets (1-f) according to Cassie-Baxter model.

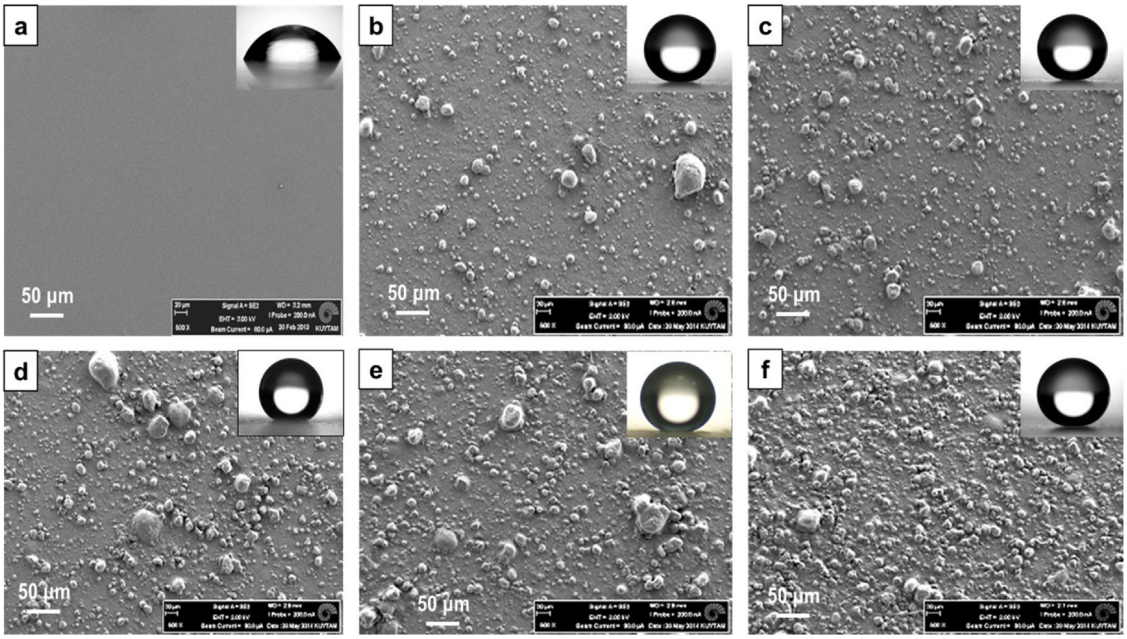

Fig. 3. SEM images of uncoated and PMMA/silica coated glass surfaces, (a) neat PMMA, (b) PMMA-SC-1, (c) PMMA-SC-2, (d) PMMA-SC-3, (e) PMMA-SC-4, and (f) PMMA-SC-5.

The highest contact angle achieved was accepted as the advancing angle. Then, the volume of the water droplet was decreased from 25 μL to 5 μL with the same rate. The lowest contact angle was recorded as the receding contact angle after the contact line between the water droplet and the surface started to decrease with a satisfactory drop shape.

3. Results and discussion

3.1. PMMA surfaces obtained by the spin-coating of PMMA/silica dispersions

Spin-coating is a simple process to produce thin films on various substrates. Fig. 3 provides the SEM images of surfaces spin-coated with increasing number of layers of PMMA/silica (1/10 by weight) dispersions in toluene together with CA images obtained on each surface.

As expected, neat PMMA coated glass surface is very smooth and featureless (Fig. 3a). On the other hand SEM image of the surface coated with one layer of PMMA/silica dispersion (PMMA-SC-1) shows surface coverage with randomly distributed and agglomerated silica particles with base diameters in 2–20 μm range (Fig. 3b). As the number of spin-coating layer increases surface density of the agglomerated silica particles increase without significant change in the particle size. Compared to smooth PMMA surface, which displays a static water contact angle (CA) of 67.5°, rough PMMA surfaces display CA values well above 150° as provided in Table 1. These results are fairly similar to those observed on surfaces produced spin-coating of polystyrene/silica dispersions [14]. As shown in Fig. 4a and b, micron-sized silica agglomerates display nanostructured surfaces. Presence of hierarchical micro-nano surface roughness is critical in obtaining superhydrophobic surfaces [1,2,6,19].

2D and 3D topographical maps of 47 × 63 μm^2 sections of PMMA-SC-5 surfaces obtained by WLI studies are reproduced in Fig. 5a and b respectively. Also provided in Fig. 5c and d are the depth profiles of this surface along (x) and (y) axes shown by the lines in Fig. 5a. Randomly distributed silica agglomerates with base diameters ranging from 2 to 20 μm, similar to those observed in SEM images, can be seen in Fig. 5a and b. Heights of the silica particles obtained from depth profiles are in 2–8 μm range.

Average surface roughness (R_a) and Wenzel roughness (r) values determined from WLI analyses are provided in Table 1 for spin-coated PMMA/silica surfaces. As can be seen in the second column of Table 1, average surface roughness (R_a) values in general are fairly high and increase from 0.40 μm to 0.77 μm with the number of spin-coatings applied. These surfaces also show fairly significant standard deviation, clearly indicating random particle sizes and distribution on these surfaces. Similarly, (r) values which are in 2.8–4.2 range are also fairly high, supporting the data on R_a. WLI and SEM images also show the presence of small number of fairly large silica agglomerates or protrusions. These results indicate presence of large area fraction of air pockets on the surface, which play critical role in achieving superhydrophobic surfaces according to Cassie-Baxter model.

Also provided in Table 1 are the static water contact angles (CA) and contact angle hysteresis (CAH) values obtained on these surfaces. As expected from high average surface roughness (R_a) values, all surfaces display very high CA values in 158–163° range, which is one of the requirements for superhydrophobic behavior. However, for a truly

Table 1
Average roughness (R_a), Wenzel roughness (r), static water contact angle (CA) and contact angle hysteresis (CAH) values of spin-coated PMMA/silica surfaces.

Sample Code	(R_a) (μm)	(r)	CA (°)	Advancing (θ_A) and Receding (θ_R) contact angles and contact angle hysteresis (CAH) values (°)		
				(θ_A)	(θ_R)	CAH
PMMA-SC-1	0.40 ± 0.16	2.94 ± 0.51	163.0 ± 0.5	165.8 ± 1.6	160.9 ± 1.3	4.9
PMMA-SC-2	0.60 ± 0.16	2.84 ± 0.34	162.9 ± 0.8	168.6 ± 1.9	160.5 ± 9.0	8.1
PMMA-SC-3	0.70 ± 0.15	3.81 ± 0.68	158.4 ± 2.7	160.2 ± 0.4	151.3 ± 1.1	8.9
PMMA-SC-4	0.65 ± 0.19	3.05 ± 1.22	160.2 ± 5.9	165.0 ± 0.6	148.6 ± 1.4	16.4
PMMA-SC-5	0.77 ± 0.27	4.17 ± 2.40	160.5 ± 1.0	162.8 ± 0.2	144.6 ± 1.8	18.2

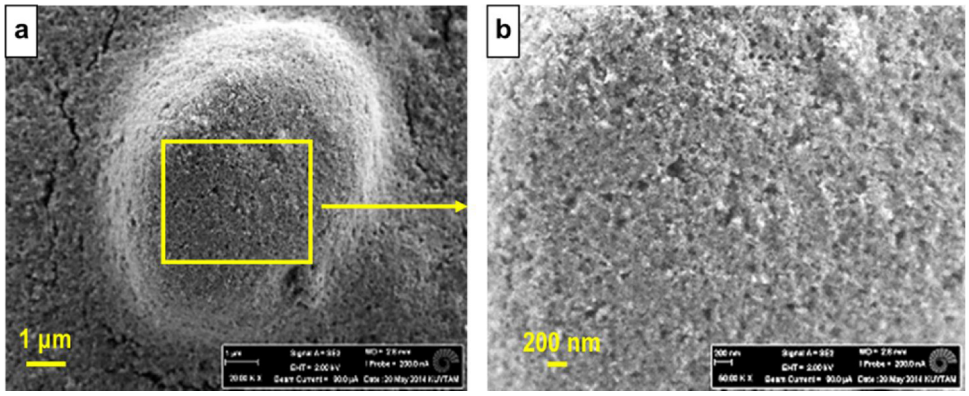

Fig. 4. SEM images of (a) micron-sized silica agglomerate on PMMA-SC-1 surface, (b) surface nanostructure of the silica agglomerate.

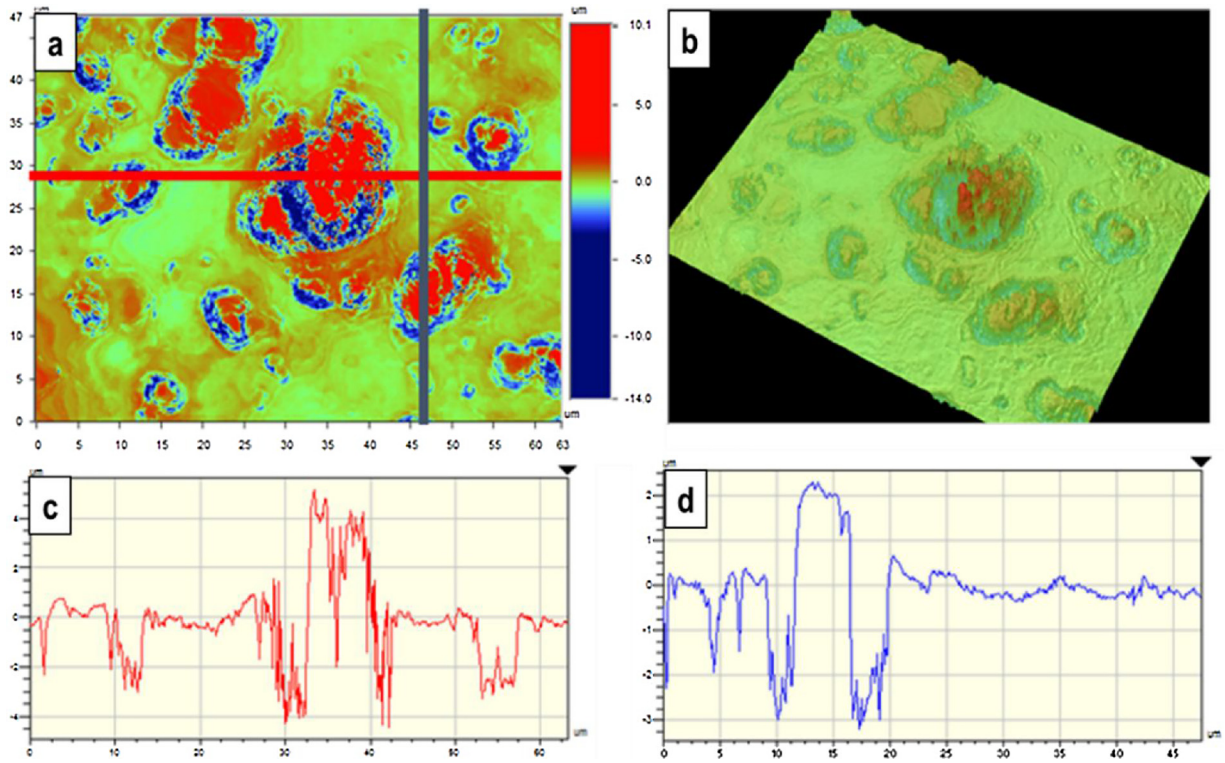

Fig. 5. (a) 2D WLI topographical map, (b) 3D WLI topographical map of the PMMA-SC-5 surface with corresponding (c) X and (d) Y height profiles.

superhydrophobic surface CAH also needs to be smaller than 10°. As can be seen in Table 1, first three samples display low CAH values, indicating that these surfaces are truly superhydrophobic. Interestingly, surfaces obtained after 4 and 5 spin-coating layers display much higher CAH values, most probably indicative of more effective pinning of the droplets on these very rough surfaces with large agglomerates.

3.2. PMMA surfaces obtained by the doctor blade coating of PMMA/silica dispersions

Doctor blade is a widely used technique for the preparation of coatings with controlled thicknesses both in laboratory scale but also in large scale commercial applications. Concentration of the solution or dispersion used and the gauge length of the doctor blade control the coating thickness. In this study we kept the concentration of PMMA/silica (1/10 by weight) dispersion constant at 5% by weight in toluene and used three different gauge lengths of 200, 125 and 50 µm, leading to approximate dry coating thicknesses of approximately 5, 3 and 1.3 µm. SEM images of the dry coated surfaces are provided in Fig. 6, together with respective CA images. When compared with the surafces obtained by spin-coating, doctor blade coatings display more homogeneous surface coverage by silica agglomerates and fairly uniform particle size distribution. As the gauge length of the doctor blade increases, average silica agglomerate sizes also increase as can be seen in SEM images in going from Fig. 6a–c.

As already discussed, WLI investigations provide fairly accurate data on the average surface roughness (R_a), roughness factor (r) and distribution and heights of the silica particles on the surface. 2D and 3D WLI images and depth profiles of PMMA-DB-50 and PMMA-DB-200 surfaces are provided in Figs. 7 and 8 respectively.

As can be seen in the 2D and 3D surface images of PMMA-DB-50 reproduced in Fig. 7a and b respectively, surface is homogeneously covered with silica agglomerates with sizes varying in a fairly narrow scale of about 2 to 5 µm, which can be deduced from the (x) and (y) axis profiles shown in Fig. 7c and d. Surface profiles given in Fig. 7c and d clearly show the heights of the silica agglomerates on PMMA-DB-50 surface to vary between 0.1 and 1.0 µm, which are much lower when compared with the spin-coated samples discussed in Section 3.1. As

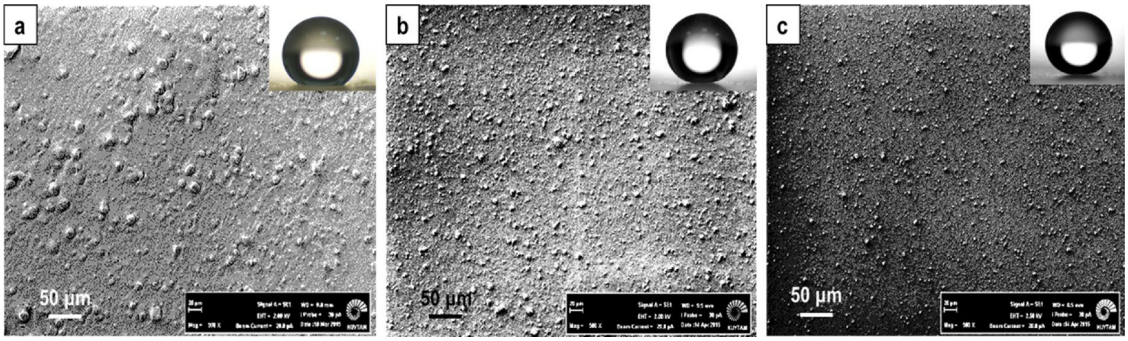

Fig. 6. SEM micrographs of doctor blade coated PMMA/silica surfaces. (a) PMMA-DB-50, (b) PMMA-DB-125 and (c) PMMA-DB-200.

expected, such low values in the heights of the silica agglomerates is directly related to the gauge length of the doctor blade used, which controls the dry coating thickness. As already mentioned, average dry coating thickness estimated for PMMA-BD-50 is approximately 1.3 µm. The heights of silica agglomerates observed are in very good agreement with the estimated coating thickness. As provided in Table 2, average surface roughness (R_a) and roughness factor (r) values obtained from WLI studies for PMMA-DB-50 are 75 ± 8 nm and 1.09 ± 0.02 respectively. These values are much lower when compared to those obtained on single layer spin-coated surface, indicating better control of the coating by doctor blade process.

Surface topography of PMMA-DB-200 coatings is quite different than that of PMMA-DB-50, clearly demonstrating the influence of gauge thickness on the structure and topography of the coated surface. As can be seen in Fig. 8a and b, sizes of the silica agglomerates in PMMA-DB-200 are in 2–10 µm range, quite larger than those on PMMA-DB-50, which is expected. More importantly, as can be seen in the depth profiles given in Fig. 8c and d, heights of the silica agglomerates also increased up to 3 µm, resulting in much higher average surface roughness of 200 ± 20 nm and a roughness factor of 1.37 ± 0.06 (Table 2). As expected, average roughness and roughness factor values increase with increasing gauge length as shown in Table 2.

Critical influence of the average surface roughness and size and height of the silica agglomerates are clearly observed on the wetting behavior of the coatings obtained. As shown in Table 2, CA of PMMA-DB-50, which has the lowest surface roughness, is 138.5° and below the critical value of 150° required for superhydrophobic behavior. CA values measured on PMMA-DB-125 and PMMA-DB-200 are 159.6 and 159.8° respectively, clearly showing the effect of increased surface roughness. Another critical requirement for a superhydrophobic surface is the value of CAH. In addition to displaying the lowest CA, PMMA-DB-50 coating surface also has a fairly high CAH of 28.9°, clearly showing that the surface obtained is not truly superhydrophobic. As shown in Table 2, as the average roughness of the coated surface increases CAH values decrease. Data provided in Table 2 support the results of previously published studies that the threshold average surface roughness value (R_a) to obtain superhydrophobic PMMA/silica surfaces is about 200 nm [12]. When the doctor blade coated PMMA/silica surfaces produced in this study are compared, only PMMA-DB-200 displays truly superhydrophobic behavior.

3.3. Determination of the area of protrusions from Cassie-Baxter equation

As clearly shown in Fig. 1 Wenzel model cannot be used to explain the conversion of an inherently hydrophilic surface, such as PMMA to superhydrophobic by the introduction of roughness. However, as we

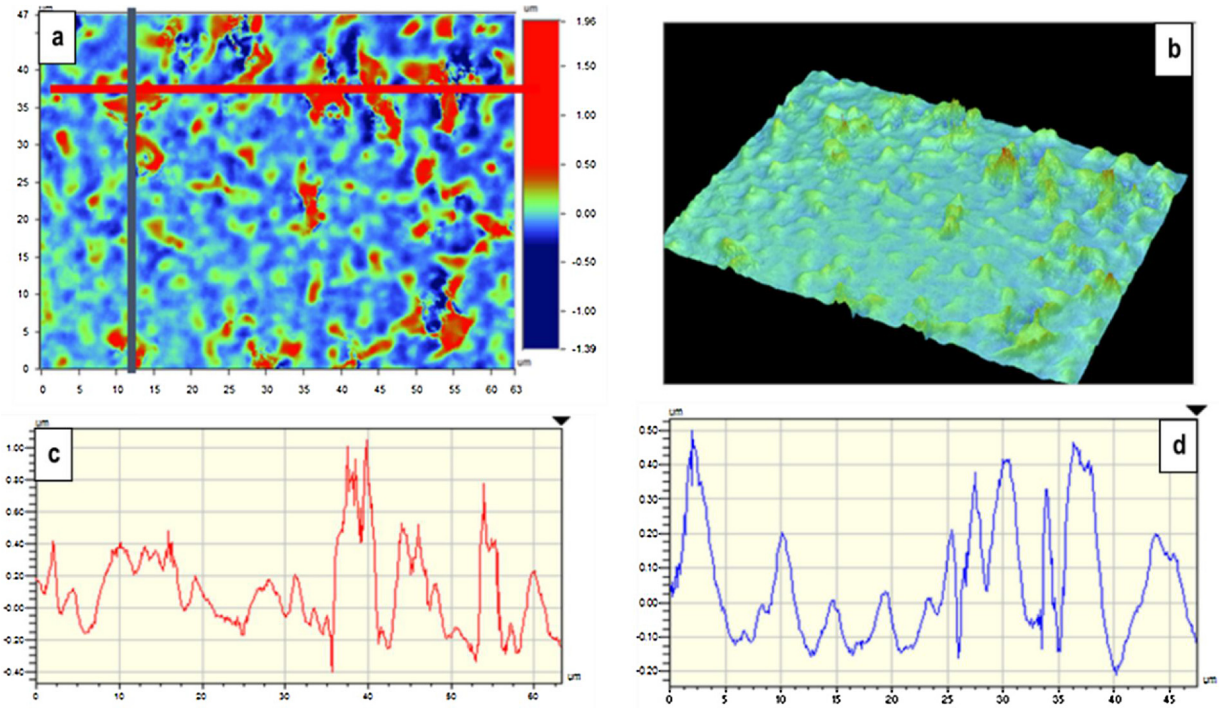

Fig. 7. 47 × 63 µm^2 WLI images of PMMA-DB-50 surface. (a) 2D and (b) 3D topographical images and corresponding surface profiles along (c) X-axis and (d) Y-axis.

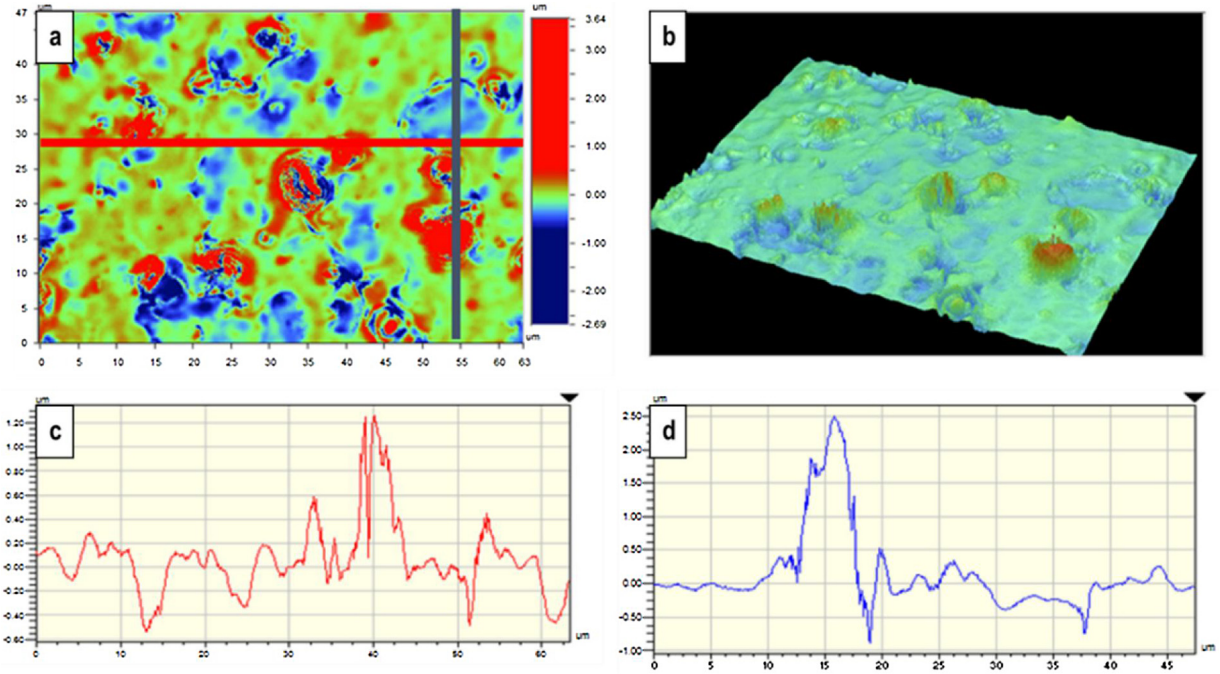

Fig. 8. 47 × 63 μm^2 WLI images of PMMA-DB-200 surface. (a) 2D and (b) 3D topographical images and corresponding surface profiles along (c) X-axis and (d) Y-axis.

Table 2
Effect of process parameters on the static, advancing and receding water contact angles, contact angle hysteresis (CAH), average arithmetic roughness (R_a), and roughness factor (r) for the PMMA-DB samples.

Sample Code	Coating thickness (μm)	R_a (nm)	(r)	CA (°)	Advancing (θ_A), Receding (θ_R) contact angles and contact angle hysteresis (CAH) values (°)		
					(θ_A)	(θ_R)	CAH
PMMA-DB-50	1.3	75 ± 8	1.09 ± 0.02	138.5 ± 3.4	142.6 ± 1.4	113.7 ± 2.4	28.9
PMMA-DB-125	3	130 ± 60	1.12 ± 0.10	159.6 ± 5.3	160.2 ± 0.4	146.9 ± 1.1	13.3
PMMA-DB-200	5	200 ± 20	1.37 ± 0.06	159.8 ± 3.4	160.7 ± 1.8	151.4 ± 1.4	9.3

Table 3
Estimation of fraction (f) and percent (%) area covered by protrusions on rough PMMA surfaces using experimentally determined static water contact angles and Cassie-Baxter equation. Coatings were prepared on smooth glass substrates using PMMA/silica (1/10 by weight) dispersions and spin-coating (SC) and doctor blade (DB) coating methods.

Sample code	CA (°)	f	(%)
PMMA-DB-50	138.5 ± 3.4	0.182	18.2
PMMA-DB-125	159.6 ± 5.3	0.045	4.5
PMMA-DB-200	159.8 ± 3.4	0.044	4.4
PMMA-SC-1	163.0 ± 0.5	0.032	3.2
PMMA-SC-2	162.9 ± 0.8	0.032	3.2
PMMA-SC-3	158.4 ± 2.7	0.051	5.1
PMMA-SC-4	160.2 ± 5.9	0.043	4.3
PMMA-SC-5	160.5 ± 1.0	0.042	4.2

have experimentally demonstrated in this study, it is possible to obtain superhydrophobic PMMA surfaces by introducing roughness, which can theoretically be explained by Cassie-Baxter approach. As a result we used Cassie-Baxter model to estimate the fraction of the surface area of protrusions (f) on the coatings obtained by spin coating and doctor blade coating of PMMA/silica (1/10 by weight) dispersions on smooth glass surfaces. The results are provided in Table 3. As can clearly be seen in Table 3, PMMA/silica (1/10 by weight) dispersions can effectively be utilized to prepare rough surfaces with very small area fraction of protrusions. These surfaces display superhydrophobic behavior, wetting behavior of which can be explained according to Cassie-Baxter model.

4. Conclusions

PMMA films and sheets display excellent clarity and high transmission of visible light. As a result they are widely used in paints and coatings and as protective panels in outdoor displays. PMMA, which is inherently a hydrophilic polymer can be wetted by water or dirt that reduces its transparency. Such problems can be avoided by preparing clear, superhydrophobic, self-cleaning coatings. In this study PMMA surfaces displaying superhydrophobic properties were prepared by spin-coating and doctor blade coating on glass substrates, using PMMA/hydrophobic silica (1/10 by weight) dispersions in toluene. Influence of the number of coating layers applied and doctor blade gauge length on topographies of the surfaces formed and their wetting behavior were investigated. Formation of dual scale, micro/nano surface structures were demonstrated by scanning electron microscopy, atomic force microscopy and white light interferometry studies. Critical influence of average surface roughness (R_a) on the superhydrophobic behavior of the surfaces formed was clearly demonstrated. Static, advancing and receding water contact angles above 150 degrees and fairly low contact angle hysteresis values clearly showed the conversion of hydrophilic PMMA surfaces to superhydrophobic. Wetting behavior of rough PMMA surfaces were explained by Cassie-Baxter model. Area fractions of protrusions and air pockets on PMMA coatings obtained by different experimental methods were also determined using Cassie-Baxter equation.

Data availability

The raw/processed data required to reproduce these findings cannot be shared at this time as the data also forms part of an ongoing study.

References

[1] P. Roach, N.J. Shirtcliffe, M.I. Newton, Progess in superhydrophobic surface development, Soft Matter 4 (2) (2008) 224–240.
[2] B. Bhushan, Biomimetics: lessons from nature – an overview, Philos. Trans. R. Soc. A-Math. Phys. Eng. Sci. 367 (1893) (2009) 1445–1486.
[3] B. Bhushan, Y.C. Jung, Natural and biomimetic artificial surfaces for superhydrophobicity, self-cleaning, low adhesion, and drag reduction, Prog. Mater. Sci. 56 (1) (2011) 1–108.
[4] K. Koch, B. Bhushan, W. Barthlott, Multifunctional surface structures of plants: an inspiration for biomimetics, Prog. Mater. Sci. 54 (2) (2009) 137–178.
[5] S. Wang, et al., Bioinspired surfaces with superwettability: new insight on theory, design, and applications, Chem. Rev. 115 (16) (2015) 8230–8293.
[6] B. Bhushan, K. Koch, Y.C. Jung, Biomimetic hierarchical structure for self-cleaning, Appl. Phys. Lett. 93 (9) (2008).
[7] G.D. Bixler, et al., Anti-fouling properties of microstructured surfaces bio-inspired by rice leaves and butterfly wings, J. Colloid Interface Sci. 419 (2014) 114–133.
[8] E. Celia, et al., Recent advances in designing superhydrophobic surfaces, J. Colloid Interface Sci. 402 (2013) 1–18.
[9] L. Yao, J. He, Recent progress in antireflection and self-cleaning technology – from surface engineering to functional surfaces, Prog. Mater. Sci. 61 (2014) 94–143.
[10] S.S. Latthe, et al., Recent progress in preparation superhydrophobic surfaces: a review, J. Surf. Eng. Mater. Adv. Technol. 2 (2012) 76–94.
[11] I. Yilgor, et al., Facile preparation of superhydrophobic polymer surfaces, Polymer 53 (6) (2012) 1180–1188.
[12] C.K. Soz, E. Yilgor, I. Yilgor, Influence of the average surface roughness on the formation of superhydrophobic polymer surfaces through spin-coating with hydrophobic fumed silica, Polymer 62 (2015) 118–128.
[13] C.K. Soz, E. Yilgor, I. Yilgor, Influence of the coating method on the formation of superhydrophobic silicone-urea surfaces modified with fumed silica nanoparticles, Prog. Org. Coat. 84 (2015) 143–152.
[14] C.K. Soz, E. Yilgor, I. Yilgor, Simple methods for the preparation of superhydrophobic polymer surfaces, Polymer 99 (2016) 580–593.
[15] R.N. Wenzel, Resistance of solid surfaces to wetting by water, Ind. Eng. Chem. 28 (8) (1936) 988–994.
[16] A.B.D. Cassie, S. Baxter, Wettability of porous surfaces, Trans. Faraday Soc. 40 (1944) 546–551.
[17] C. Neinhuis, W. Barthlott, Characterization and distribution of water-repellent, self-cleaning plant surfaces, Ann. Bot. 79 (6) (1997) 667–677.
[18] T. Wagner, C. Neinhuis, W. Barthlott, Wettability and contaminability of insect wings as a function of their surface sculptures, Acta Zool. 77 (3) (1996) 213–225.
[19] W. Barthlott, C. Neinhuis, Purity of the sacred lotus, or escape from contamination in biological surfaces, Planta 202 (1) (1997) 1–8.
[20] T. Onda, et al., Super-water-repellent fractal surfaces, Langmuir 12 (9) (1996) 2125–2127.
[21] H.Y. Erbil, C.E. Cansoy, Range of applicability of the Wenzel and Cassie-Baxter equations for superhydrophobic surfaces, Langmuir 25 (24) (2009) 14135–14145.
[22] C.W. Extrand, Model for contact angles and hysteresis on rough and ultraphobic surfaces, Langmuir 18 (21) (2002) 7991–7999.
[23] C.W. Extrand, Contact angles and hysteresis on surfaces with chemically heterogeneous islands, Langmuir 19 (9) (2003) 3793–3796.
[24] L.C. Gao, T.J. McCarthy, How Wenzel and Cassie were wrong, Langmuir 23 (7) (2007) 3762–3765.
[25] L.C. Gao, T.J. McCarthy, Wetting 101 degrees, Langmuir 25 (24) (2009) 14105–14115.
[26] D.C. Pease, The significance of the contact angle in relation to the solid surface, J. Phys. Chem. 49 (2) (1944) 107–110.
[27] M. Nosonovsky, On the range of applicability of the Wenzel and Cassie equations, Langmuir 23 (19) (2007) 9919–9920.
[28] A. Marmur, E. Bittoun, When Wenzel and cassie are right: reconciling local and global considerations, Langmuir 25 (3) (2009) 1277–1281.